NFATc2 (NFAT1) Assists BCR-Mediated Anergy in Anti-Insulin B Cells

Rachel H. Bonami[a], **William T. Wolfle**[a], **James W. Thomas**[a,b], and **Peggy L. Kendall**[b,c]

[a]Division of Rheumatology and Immunology, Department of Medicine, Vanderbilt University, MCN T3113, 21st Ave. S., Nashville, TN 37232, U.S.A

[b]Department of Pathology, Microbiology, and Immunology, Vanderbilt University, MCN T3113, 21st Ave. S., Nashville, TN 37232, U.S.A

[c]Division of Allergy, Pulmonary, and Critical Care, Department of Medicine, Vanderbilt University, MCN T3113, 21st Ave. S., Nashville, TN 37232, U.S.A

Abstract

NFAT transcription factors play critical roles in both the activation and repression of T and B lymphocyte responses. To understand the role of NFATc2 (NFAT1) in the maintenance of tolerance for anti-insulin B cells, functionally inactive NFATc2 (NFATc2$^{-/-}$) was introduced into C57BL/6 mice that harbor anergic anti-insulin 125Tg B cells. The production and peripheral maturation of anti-insulin B cells into follicular and marginal zone subsets was not altered by the absence of functional NFATc2. Surface B cell receptor expression levels, important for tonic signaling and altered by anergy, were not altered in any spleen B cell subset. The levels of anti-insulin antibodies were not different in 125Tg/B6/NFATc2$^{-/-}$ mice and the anti-insulin response remained silenced following T cell dependent immunization. However, studies addressing *in vitro* proliferation reveal the anergic state of 125Tg B cells is relieved in 125Tg/B6/NFATc2$^{-/-}$ B cells in response to BCR stimulation. In contrast, anergy is not released in 125Tg/B6/NFATc2$^{-/-}$ B cells following stimulation with anti-CD40. The relief of anergy to BCR stimulation in 125Tg/B6/NFATc2$^{-/-}$ B cells is associated with increased transcription of both NFATc1 and NFATc3 while expression of these NFATs does not change in anti-IgM stimulated 125Tg/B6/NFATc2$^{+/+}$ B cells. The data suggest that NFATc2 plays a subtle and selective role in maintaining anergy for BCR stimulation by repressing the transcription of other NFAT family members.

Keywords

B Cell; NFAT; Autoimmunity; Tolerance; Insulin; Signaling

Corresponding author: James W. Thomas, james.w.thomas@vanderbilt.edu, (615) 322-4746, MCN T3113, 21st Ave. S., Nashville, TN 37232, U.S.A.

1. Introduction

Insulin is a 5800 Da protein that is synthesized, stored, and secreted by the pancreatic islets of all mammals. Administration of the hormone is life saving for individuals with type 1, or insulin dependent, diabetes mellitus (T1D), and is also used for metabolic control in many patients with type 2 diabetes. Although insulin was once considered too small to induce specific immunity, a large body of clinical and experimental data clearly demonstrates that immune responses to insulin arise in a variety of circumstances. Antibodies (Ab) to insulin are almost universal in treated patients and insulin autoantibodies are recognized as part of the natural autoantibody repertoire (Coutinho *et al.*, 1995; van Haeften, 1989). In contrast to common insulin Ab that rarely cause symptoms, dramatic insulin resistance occurs as part of the insulin autoimmune syndrome in which high titers of insulin Ab require massive dosages of insulin to maintain metabolic control. The insulin autoimmune syndrome may accompany an underlying autoimmune disorder such as lupus erythematosus or it may occur as a primary immunological disorder (Blackshear *et al.*, 1983; Lupsa *et al.*, 2009). The most common autoimmune disorder associated with insulin autoantibodies is type 1 diabetes (T1D). Autoantibodies to insulin arise asymptomatically during the prodrome of T1D and are biomarkers of the autoimmune process that destroys pancreatic beta cells and causes diabetes (Palmer *et al.*, 1983; Eisenbarth *et al.*, 2002). Although Ab are not considered primary mediators of beta cell destruction, autoantibodies to insulin and other beta cell autoantigens are critically important tools for detection and early intervention in T1D. The clinical features of insulin immunity and autoimmunity indicate that the insulin molecule challenges the mechanisms that maintain tolerance for self-proteins.

To better understand how tolerance is maintained for anti-insulin B lymphocytes, our laboratory generated mice that harbor VH or VL genes from anti-insulin mAb125 as BCR (IgM) transgenes. Mab125 was obtained from the primary immune response of a non-autoimmune BALB/c mouse and binds rodent insulin with an affinity of 1×10^{-7} M. In contrast to transgenic models that employ high affinity BCRs, this model assesses the fate and function of B cells whose BCRs represent an early or primary immune response. Mice that carry both VH125 and Vκ125 transgenes (125Tg) have a large population of insulin-binding B cells (Rojas *et al.*, 2001). Studies in this model demonstrate that a majority of BCRs on anti-insulin B cells in the periphery are occupied by endogenous insulin, and the initial encounter with insulin has been tracked to early B cell development in the bone marrow parenchyma (Henry-Bonami *et al.*, 2013). In contrast to high-affinity models of B cell tolerance, insulin-binding B cells are not developmentally arrested; they enter mature follicular (FO) and marginal zone (MZ) compartments, with an increase in MZ B cells. Although anti-insulin B cells reside in mature subsets, their ability to produce Ab following T cell-dependent immunization is silenced (Rojas *et al.*, 2001). Similarly, *in vitro* studies on freshly isolated anti-insulin B cells demonstrate impaired lymphocyte proliferation following stimulation through the BCR, TLR4 and CD40 (Acevedo-Suarez *et al.*, 2005). This form of "split" tolerance, in which functional silencing and anergy are separated from alterations in B cell development, is similarly maintained in both non-autoimmune C57BL/6 and autoimmune nonobese diabetic (NOD) mice (Acevedo-Suarez *et al.*, 2005).

The mechanisms that maintain tolerance for anti-insulin B cells also differ from the high-affinity models of B cell tolerance. Anti-insulin B cells do not demonstrate elevated basal levels of intracellular calcium present in the hen egg lysozyme (HEL)/anti-HEL BCR transgenic model, and they do not have impaired tyrosine kinase substrate phosphorylation following BCR stimulation with anti-IgM (Acevedo-Suarez *et al.*, 2006). However, intracellular levels of inositol 1, 4, 5-triphosphate are increased, and NFATc1 levels are reduced in 125Tg/B6 B cells. In contrast to antigen-naïve B cells, anti-insulin B cells from the spleen are unable to signal calcium transients in response to insulin (Acevedo-Suarez *et al.*, 2006; Kendall *et al.*, 2013). Further, bone marrow cultures that investigate the encounter of naïve immature anti-insulin B cells with insulin show the induction of anergy is associated with reduced intracellular mobilization of calcium (Henry *et al.*, 2009). Immature B cell proliferation to anti-CD40 is blunted by insulin antigen exposure or calcineurin inhibition, also indicating a possible role for NFAT in maintaining anergy (Henry *et al.*, 2009). Together, these data suggest that low amplitude, calcium-mediated signals play a key role in the induction and maintenance of tolerance for anti-insulin B cells.

Low amplitude calcium signaling is recognized to activate calcineurin phosphatase, which dephosphorylates NFATs and allows nuclear entry of the cytoplasmic transcription factor without perturbation of other pathways (Dolmetsch *et al.*, 1997). NFATc2 (also known as NFAT1) is recognized to play a key role in regulating tolerance in T cells and is necessary for induction of anergy with anti-CD3 or ionomycin *in vitro* (Macian *et al.*, 2002). Using bone marrow chimeras in the high-affinity HEL/anti-HEL model, NFATc2 was found to have a role in regulating B cell tolerance (Barrington *et al.*, 2006). In that study, B cell anergy was relieved in NFATc2$^{-/-}$ mice as evidenced by increased amounts of circulating autoantibody, increased numbers of mature B cells and increased responses to allo-T cell help (Barrington *et al.*, 2006). However, a role for NFATs in inducing B cell tolerance in the same model has been questioned by the observation that features of tolerance (reduced surface IgM and autoantibody production) are not changed in the absence of calcineurin B (Winslow *et al.*, 2006).

The contributions of NFATc2 to tolerance may differ depending on the status of signals that maintain tolerance for different autoreactive B cells. To determine how NFATc2 contributes to tolerance maintained by low amplitude calcium signaling, anti-insulin BCR transgenic mice (125Tg) were intercrossed with mice in which the Rel homology (DNA binding) domain of NFATc2 is inactivated (termed NFATc2$^{-/-}$ mice) (Hodge *et al.*, 1996; Barrington *et al.*, 2006; Xanthoudakis *et al.*, 1996). Studies in these mice demonstrate that NFATc2 does not regulate the developmental fate of anti-insulin B cells that enter the mature repertoire and its presence is not required to maintain anergy to anti-CD40 stimulation *in vitro*, or for functional silencing of T cell-dependent responses in 125Tg/B6 mice. However, NFATc2 contributes to the maintenance of anergy via signaling through anti-insulin BCRs. Anti-insulin 125Tg/B6 B cells lacking functional NFATc2 generate near normal proliferative responses to BCR engagement with anti-IgM. This relieved anergy in 125Tg/B6/NFATc2$^{-/-}$ B cells is associated with heightened transcription of NFATc1 and NFATc3 following anti-IgM stimulation. These studies support a role for NFATc2 in

maintaining tolerance for BCR signaling pathways by its regulation of expression of other NFATs.

2. Materials and Methods

2.1 Animals

All mice were backcrossed at least 20 generations onto the C57BL/6 (B6) background. 125Tg mice harbor non-targeted anti-insulin heavy and light chain transgenes that produce an anti-insulin BCR (Rojas *et al.*, 2001). NFATc2$^{-/-}$ mice were a kind gift from Anjana Rao (Harvard University, Boston, MA) (Xanthoudakis *et al.*, 1996). 125Tg/B6 were intercrossed with NFATc2$^{-/-}$ to generate 125Tg/B6/NFATc2$^{-/-}$ mice. 7–28 week old male and female mice were used in all experiments. All studies were approved by the AAALAC-certified Institutional Animal Care and Use Committee of Vanderbilt University and mice were housed in specific pathogen free conditions.

2.2 Immunization and Antibody Detection

125Tg/B6 and B6 NFATc2$^{+/+}$ or NFATc2$^{-/-}$ mice were immunized with 50 μg beef insulin in CFA subcutaneously at the base of the tail. Sera were obtained pre-immunization and 2 weeks post-immunization from each mouse. ELISA was used to detect insulin-specific antibodies, as has been previously described (Kendall *et al.*, 2004). Briefly, the O.D. 405 nm of wells incubated with >100-fold excess insulin in solution was subtracted from the O.D. 405 nm of uninhibited parallel wells to calculate insulin-specific binding. Goat anti-mouse IgM-alkaline phosphatase or goat anti-mouse IgG-alkaline phosphatase (Southern Biotech) were used to detect serum antibody bound to the insulin-coated ELISA plate.

2.3 Cell Isolation and Flow Cytometry

Splenocytes were macerated in Hanks balanced salt solution (HBSS) + 10% fetal bovine serum (FBS) (HyClone) and red blood cells were lysed using Tris-buffered NH_4Cl. Lavage with HBSS was used to isolate peritoneal cavity cells. Ab reagents reactive with B220 (6B2), IgM^a (DS-1), IgM^b (AF6-78), CD5 (53-7.3), CD21 (7G6), CD23 (B3B4), or 7-aminoactinomycin D (BD Biosciences) were used for flow cytometry. Human insulin (Sigma-Aldrich) was biotinylated at pH 8 in bicine buffer using biotin N-hydroxysuccinimide ester (Sigma-Aldrich) and detected with fluorochrome-labeled streptavidin (BD Biosciences).

2.4 B Lymphocyte Proliferation

Splenocytes were isolated as above and magnetic activated cell sorting (MACS) was used to deplete CD43-expressing cells using LS columns (Miltenyi). Sorted B cells were plated at 2×10^{-5} cells/well in complete RPMI 1640 media (Invitrogen Life Technologies) containing 10% FBS, glutamine, gentamicin, and 2×10^{-5} M 2-ME (Invitrogen Life Technologies) in 96-well, flat-bottom plates (Corning). Stimuli include anti-IgM F(ab')$_2$ (Jackson ImmunoResearch Laboratories) and anti-CD40 (HM40-3; BD Biosciences) and were added on day 0. Cells were pulsed with 1 μCi of [^{3}H]thymidine (NEN) per well on day 2 and were harvested on day 3 using a semi-automated cell harvester (Skatron), at which point

scintillation counting was used to measure [^{3}H]Thymidine incorporation. The average of triplicate wells ± SD is reported.

2.5 Quantitative Real-Time PCR

Spleen B cells were purified by CD43 MACS depletion as above and were resuspended at 2×10^6 cells/mL in RPMI 1640 + 0.1% FBS. Cells were then incubated with or without 10 μg/mL anti-IgM F(ab')$_2$ for 1h at 37°C. RNA was extracted using an RNAqueous Micro Kit (Ambion). First-strand cDNA was synthesized using SuperScript II (Invitrogen Life Technologies), according to the manufacturer's instructions and was used as a template in real-time PCR using Platinum SYBR Green qPCR SuperMix-UDG (Invitrogen Life Technologies) with an iCycler (Bio-Rad). RT^2 qPCR primer assays for mouse Nfatc1 (PPM04560F), Nfatc2 (PPM045555E) and Nfatc3 (PPM04561F) (SABiosciences) were used according to the recommended protocol. The efficiency of these primers was 97% and they generate amplicons from all major splice variants. Each set of samples was normalized using CD19 as a B cell specific gene using 2^(CD19 Ct-NFAT Ct). CD19 primers: FWD 5' GTGGCCAAAGCGTCCATC 3' and REV 5' GAGAGCACATTCCCGTAC 3'. Plasmids containing NFATc1, NFATc2, and NFATc3 (a gift from H. Scott Baldwin, Vanderbilt University, Nashville, TN) and CD19 (a gift from Tom Tedder, Duke University, Durham, NC) were employed as controls.

3. Results

3.1 Anti-insulin B cell production and peripheral maturation is not altered in NFATc2 defective mice

In contrast to high-affinity models of B cell tolerance, such as sHEL/anti-HEL, anti-insulin B cells are not subject to developmental arrest. Rather, 125Tg B cells are competent to enter mature peripheral compartments where they populate the MZ subset in increased numbers (Acevedo-Suarez *et al.*, 2005). NFATc2 has been shown to contribute to developmental alterations in sHEL/anti-HEL mice (Barrington *et al.*, 2006). To investigate its role in the development of anti-insulin B cells, the same transcriptionally inactivated NFATc2 used in the HEL studies [NFATc2$^{-/-}$ (Barrington *et al.*, 2006)] was introduced into wild type (B6) and anti-insulin 125Tg mice on the C57BL/6 (B6) background. Flow cytometry was used to investigate the frequency of B cells (B220$^+$ lymphocytes) in the presence or absence of functional NFATc2. As previously reported (Rojas *et al.*, 2001), >95% of B cells bind insulin in 125Tg/B6/NFATc2$^{+/+}$ mice, as confirmed by biotinylated insulin staining, whereas this population is virtually absent in B6/NFATc2$^{+/+}$ mice (Fig. 1A). As expected, the frequency of insulin-binding B cell is not altered by NFATc2$^{-/-}$ (Fig. 1A). The percentage of spleen B cells in B6/NFATc2$^{-/-}$ mice is slightly reduced compared to B6/NFATc2$^{+/+}$ mice (44 ± 12% vs. 52 ± 11%, p < 0.05), however no significant difference in B cell numbers is observed (49 ± 13 × 10^6 vs. 45 ± 10 × 10^6, p = 0.45, Fig. 1B–C, Table 1–2). The frequency or number of splenic B cells is not different in 125Tg/B6/NFATc2$^{-/-}$ vs. 125Tg/B6/NFATc2$^{+/+}$ mice (32 ± 10% vs. 32 ± 9%, p = 0.96 and 20 ± 10 × 10^6 vs. 19 ± 9 × 10^6 p = 0.74, respectively, Fig. 1B–C, Table 1–2). The reduced production of B cells in 125Tg/B6 mice is typical of BCR transgenics with pre-rearranged VH segments (Goodnow,

1992), regardless of the presence or absence of NFATc2. These data suggest that loss of functional NFATc2 does not alter the production of anti-insulin B cells in 125Tg/B6 mice.

To investigate peripheral maturation of B cells that enter the spleen from the bone marrow, spleen cells gated on B220^{+} lymphocytes were further identified for expression of CD21 and CD23. The levels of these co-receptor molecules delineate transitional (T1, CD21^{low} CD23^{low}), T2/FO (CD21^{low} CD23^{high}), and MZ (CD21^{high} CD23^{low}) B cells. As the transgene only encodes IgM in 125Tg B cells (Rojas *et al.*, 2001), IgD cannot be used to further define these populations. Representative flow cytometry dotplots are shown in Fig. 2A, and the results from multiple mice are summarized in Fig. 2B–C. Consistent with previous reports (Acevedo-Suarez *et al.*, 2005), MZ B cells are increased ($35 \pm 15\%$ vs. $7 \pm 2\%$) and T2/FO B cells are decreased (52 ± 14 vs. $77 \pm 4\%$) in anti-insulin 125Tg/B6/NFATc2^{+/+} vs. B6/NFATc2^{+/+} mice. NFATc2 deficiency does not alter the percentage or number of T2/FO or MZ B cells in 125Tg/B6/NFATc2^{−/−} or B6/NFATc2^{−/−} mice (Fig. 2A–C, Table 1–2). Further breakdown of the CD21^{low} CD23^{high} subset into T2 (IgM^{hi}) and FO (IgM[mid]) B cell subsets also shows no effect of NFATc2 deficiency on subset frequency or number in 125Tg/B6 of B6 mice (not shown). These data suggest that B cell developmental subset proportions are not changed by NFATc2 deficiency in B6 or 125Tg/B6 mice.

B1a cells in the peritoneal cavity are often polyreactive and are an important source of natural antibodies. To test whether differences exist in the frequency of B1a B cells that could impact autoantibody production, flow cytometry was used to assess this population in B6 and 125Tg/B6 NFATc2^{+/+} or NFATc2^{−/−} mice. The frequency of B1a cells is low or absent in 125Tg/B6 mice ($2.9 \pm 2.5\%$), as has been previously reported (Rojas *et al.*, 2001), and was not restored by the loss of functional NFATc2 ($5.1 \pm 4.7\%$, p = 0.30, Fig. 2D–F and Table 3). The numbers and percentages of B1a B cells were also unaffected by the absence of NFATc2 in the B6 polyclonal repertoire ($29 \pm 9\%$ vs. $29 \pm 9\%$, p = 0.95, Fig. 2D–F and Table 3). These data show that the reduced B1a compartment in anti-insulin 125Tg/B6 mice is not rescued by loss of functional NFATc2.

3.2 BCR surface expression is not altered by NFATc2 deficiency

Downregulation of surface BCR is a characteristic of anergic B cells that results in changes to BCR tonic signaling (Bell and Goodnow, 1994). To test whether loss of functional NFATc2 may change BCR proximal signaling, and potentially tolerance maintenance, by altering surface IgM levels, IgM mean fluorescence intensity (MFI) was measured in spleen subsets of B6 and 125Tg/B6 NFATc2^{+/+} or NFATc2^{−/−} mice using flow cytometry. T1, T2/FO, and MZ subsets were identified as in Fig. 2. The relative IgM expression was calculated for each B cell subset by dividing the 125Tg/B6/NFATc2^{−/−} IgM MFI by 125Tg/B6/NFATc2^{+/+} IgM MFI; 125Tg/B6/NFATc2^{+/+} expression was normalized to 100%. The same analysis was performed for B6 B cells. Relative IgM surface expression was not altered by NFATc2 deficiency in either B6 or 125Tg/B6 mice (Fig. 3).

3.3 T-dependent immune response to insulin remains functionally silenced in 125Tg/B6 NFATc2-defective mice

To assess the functional status of anti-insulin B cells in the absence of NFATc2, insulin Ab were measured in naïve mice, and following T cell-dependent (TD) immunization. Circulating Ab in 125Tg/B6 mice includes a small fraction of IgM anti-insulin Ab derived from the transgene (Rojas *et al.*, 2001). The levels of these natural-like insulin autoantibodies were not different at baseline in 125Tg/B6/NFATc2$^{-/-}$ (O.D.$_{405}$ = 0.30 ± 0.21) vs. 125Tg/B6/NFATc2$^{+/+}$ mice (O.D.$_{405}$ = 0.28 ± 0.14, p = 0.76, Fig. 4A). Beef insulin immunization in CFA was then used to generate potent T cell help in B6 (H-2^b) mice (Keck, 1975). As 125Tg/B6 B cells are not competent to class switch, the change in insulin specific IgM was measured by ELISA in 125Tg/B6/NFATc2$^{+/+}$ and 125Tg/B6/NFATc2$^{-/-}$ mice. The results show that 3/9 125Tg/B6/NFATc2$^{+/+}$ and 3/7 125Tg/B6/NFATc2$^{-/-}$ mice increased IgM anti-insulin Ab appreciably above the pre-immune background following immunization (Fig. 4A). The pre-immune Ab levels did not predict subsequent TD responses. These responses are weak and only 3 mice in each group doubled pre-existing IgM anti-insulin Ab. For both groups, mice that did not respond to immunization not only failed to increase anti-insulin IgM, but anti-insulin IgM actually decreased pre-immune values more than 50% (Fig. 4A). These findings demonstrate the complex nature of B cell tolerance at low affinity for an autoantigen with variable physiologic concentrations.

Overall, functional silencing of anti-insulin B cells in the 125Tg model is maintained similarly in the presence or absence of functional NFATc2. The fixed IgM transgene in 125Tg/B6 mice, however, does not reflect the IgG response that routinely accompanies insulin immunity. Therefore, the IgG anti-insulin response was investigated in B6/NFATc2$^{+/+}$ and B6/NFATc2$^{-/-}$ mice following TD immunization. These mice do not have pre-immune insulin specific antibodies (Fig. 4B). Both B6/NFATc2$^{+/+}$ (4/4) and B6/NFATc2$^{-/-}$ (5/6) mice showed an increase in insulin-specific IgG post-immunization (Fig. 4B, p < 0.01, p < 0.01, respectively). The IgG anti-insulin response following immunization was significantly less in B6/NFATc2$^{-/-}$ mice (O.D.$_{405}$ = 0.4 ± 0.28) than in B6/NFATc2$^{+/+}$ mice (O.D.$_{405}$ = 0.96 ± 0.38), p < 0.05. While these data do not support a major role for NFATc2 in regulating insulin immunity, these experiments include defective NFATc2 in both T and B cells, and this additional complexity may obscure a role for the transcription factor in B cells.

3.4 NFATc2 contributes to BCR-mediated anergy in 125Tg/B6 B cells

B cells from 125Tg/B6 mice are anergic to B cell mitogens (Acevedo-Suarez *et al.*, 2005). To test the contribution of NFATc2 to anergy, we assessed proliferative responses by measuring [3H]Thymidine uptake of B cells purified from B6 and 125Tg/B6 NFATc2$^{+/+}$ or NFATc2$^{-/-}$ mice (Figure 5). Consistent with previously published results (Hodge *et al.*, 1996), the lack of functional NFATc2 in B6 B cells results in a modest increase in B cell proliferation following BCR engagement with F(ab')$_2$ anti-IgM (Fig. 5A). Anti-insulin 125Tg/B6 B cells are anergic to stimulation through their BCR. However, when functional NFATc2 was absent in 125Tg/B6 B cells, proliferation was restored to near normal levels (Fig. 5A). The responses were fully restored at lower concentrations of anti-IgM and were 75% restored when 10 μg/ml of anti-IgM was used. Insulin stimulation did not elicit

proliferation in either cognate (125Tg/B6) or non-cognate (B6) B cells, regardless of NFATc2 functional status (Fig. 5B). These findings are consistent with the anergic status of 125Tg/B6 B cells (Acevedo-Suarez *et al.*, 2005), and demonstrate the absence of hormonal effects on proliferation independent of the BCR. When similar studies were done using anti-CD40 as a surrogate for T cellmediated B cell proliferation, the outcome was different. B cells purified from B6 mice proliferated in response to anti-CD40, independently of the presence or absence of NFATc2 (Fig. 5C). In contrast to the findings using anti-IgM, the anergic state of 125Tg/B6 B cells was sustained following anti-CD40 stimulation in the absence of NFATc2. The findings suggest that NFATc2 contributes to anergy that is maintained through the anti-insulin 125Tg BCR. The absence of functional NFATc2, however, does not alter the anergic state in the response to anti-CD40.

3.5 Lifting anergy from 125Tg/B6/NFATc2$^{-/-}$ B cells is associated with increased expression of NFATc1 and NFATc3

To investigate the mechanisms that regulate the anergic state of anti-insulin B cells, the expression of mRNA from different NFATs was measured in purified B6 and 125Tg/B6 B cells that contain or lack functional NFATc2 using real-time PCR. The relative expression of *NFATc1*, *NFATc2*, and *NFATc3* under baseline (unstimulated) conditions and following stimulation with anti-IgM was compared to levels of *CD19* mRNA. Although trends were observed, no statistical differences in amounts of individual *NFAT* mRNAs were detected in unstimulated B cells from 125Tg/B6 (A) or B6 (B) mice that contained or lacked functional NFATc2 (Fig. 6). Anti-IgM stimulation led to an increase in *NFATc1* in B6/NFATc2$^{+/+}$, but not 125Tg/B6/NFATc2$^{+/+}$ B cells. However, the ability of 125Tg/B6/NFATc2$^{-/-}$ B cells to increase *NFATc1* in response to BCR stimulation was enhanced, as *NFATc1* levels increased >18X (Fig. 6). This dramatic change in *NFATc1* expression was also statistically greater than the increase in B6/NFATc2$^{-/-}$ B cells ($p < 0.05$). *NFATc3* levels in 125Tg/B6/NFATc2$^{-/-}$ B cells also increased in response to BCR stimulation relative to anergic 125Tg/B6/NFATc2$^{+/+}$ B cells ($p < 0.01$, Fig. 6). The data also show that *NFATc2* mRNA is still detected when its DNA binding (Rel homology) domain is deleted. Levels of *NFATc2* mRNA change minimally, a finding consistent with previous work showing that NFATc2 is constitutively expressed (Bhattacharyya *et al.*, 2011; Chuvpilo *et al.*, 1999). The findings suggest that in the absence of functional NFATc2, engagement of the 125Tg BCR with anti-IgM induces an increase in *NFATc1* and *NFATc3* transcription. Thus, the reversal of anergy following BCR stimulation in 125Tg/B6/NFATc2$^{-/-}$ B cells is associated with heightened transcription of other NFATs, including *NFATc1*, a factor that is recognized to support proliferation and suppress death in B cells (Bhattacharyya *et al.*, 2011).

4. Discussion

B cells that harbor anti-insulin transgenes (125Tg) are maintained in a functionally inactive or anergic state (Rojas *et al.*, 2001). In contrast to high-affinity models of B cell tolerance, the tolerant state of anti-insulin B cells does not arrest their maturation into FO and MZ subsets, and tyrosine kinase substrate phosphorylation is preserved following BCR stimulation with anti-IgM (Acevedo-Suarez *et al.*, 2006). Although intracellular Ca^{++} is not elevated in 125Tg/B6 B cells, reduced total NFATc1 suggests that low amplitude Ca^{++}

signaling may mediate this form of low affinity tolerance (Acevedo-Suarez *et al.*, 2006; Dolmetsch *et al.*, 1997). NFATc2$^{-/-}$ mice have a targeted deletion of the Rel homology domain resulting in a protein that does not bind DNA, and studies of this disruption suggest that NFATc2 has a repressive effect on T and B lymphocytes (Hodge *et al.*, 1996; Barrington *et al.*, 2006; Xanthoudakis *et al.*, 1996).

Studies reported here examine how the transcription factor NFATc2 (NFAT1) contributes to tolerance for anti-insulin B cells. We find that production and development of anti-insulin B cells do not differ when 125Tg mice are rendered NFATc2 defective. 125Tg/B6/NFATc2$^{-/-}$ mice phenocopy 125Tg/B6/NFATc2$^{+/+}$ mice, including modestly reduced numbers of total B cells, increased MZ B cells, decreased FO B cells, and absent peritoneal B1a B cells, relative to B6 mice (Figures 1–2). Surface IgM levels are not altered by loss of NFATc2 (Fig. 3). Basal amounts of insulin antibody and T-dependent Ab responses are not different in 125Tg/B6/NFATc2$^{-/-}$ mice (Fig. 4). Although CFA-insulin immunization induces a "leaky" response in some 125Tg mice, the functional loss of NFATc2 in 125Tg/B6/NFATc2$^{-/-}$ mice does not significantly alter either the number of mice responding or the amount of antibody produced in response to this T-dependent immunization. Despite preserving tolerance to limit insulin Ab production, loss of NFATc2 relieves the anergic state of 125Tg/B6 B cells by restoring proliferation following BCR stimulation with anti-IgM (Fig. 5). In contrast to the anti-IgM response, anergy is unaffected in the anti-CD40 response of 125Tg/B6/NFATc2$^{-/-}$ mice. The relief of anergy in 125Tg/B6/NFATc2$^{-/-}$ B cells following BCR stimulation is associated with an increase in transcription of both *NFATc1* and *NFATc3* while expression of these *NFATs* does not change in anti-IgM treated 125Tg/B6/NFATc2$^{+/+}$ B cells (Figure 6). The overall data suggest that NFATc2 plays a selective role in maintaining anergy mediated through the BCR of anti-insulin B cells by repressing the transcriptional expression of other NFAT family members. This subtle mechanism does not appreciably alter the production and development of anti-insulin B cells nor does it regulate T cell-dependent pathways of B cell activation.

The modest and selective effect of NFATc2 on tolerance in anti-insulin B cells is somewhat unexpected given the recognized repressive actions of NFATc2 on both T and B lymphocytes (Hodge *et al.*, 1996; Macian *et al.*, 2002; Barrington *et al.*, 2006; Xanthoudakis *et al.*, 1996). These data would predict elevated anti-insulin IgG responses in B6/NFATc2$^{-/-}$ mice. Despite this, immunized B6/NFATc2$^{-/-}$ mice showed significantly lower levels of anti-insulin IgG than B6/NFATc2$^{+/+}$ mice (Fig. 4). It is important to note that NFATc2 function is also impaired in other immune cell types, including T lymphocytes, which impact complex biological responses *in vivo*. The *in vivo* phenotype of NFATc2 deficiency was more pronounced in BALB/c mice, with follicular B cell expansion and splenomegaly (Hodge, *et al.*, 1996). However, the published *in vitro* responses of NFATc2-defective BALB/c to B cell mitogens (Hodge, *et al.*, 1996) are similar to those in studies reported here that use B6 mice (Fig. 5). Thus, NFATc2-defective mice have both context-dependent and cell-specific effects that will be further impacted by the autoimmune status of our anti-insulin model.

The effect of NFATc2 on tolerance was previously investigated using the anti-HEL BCR/ soluble HEL model. Functional loss of NFATc2 (NFAT1) increased basal levels of serum

anti-HEL Ab improved Ab responses to allo-T cell help, thus relieving immune tolerance (Barrington *et al.*, 2006). In contrast, the studies presented here show that basal levels of anti-insulin antibody were not increased, and T-dependent immune responses were not restored by loss of NFATc2 in anti-insulin 125Tg mice (Fig. 4). B cell proliferation to anti-CD40, which mimics T cell help, was also not restored by NFATc2 loss in anergic 125Tg mice (Fig. 5). The differences in NFATc2's contribution to tolerance in anti-HEL compared to anti-insulin B cells may reflect the more profound state of tolerance in the HEL model in which B cell survival and B cell signaling pathways are more impaired. Thus, signals delivered by different BCR self-antigen interactions may establish unresponsive states in which NFATc2 has different effects. However, other studies show that specific deletion of calcineurin b1 in the same HEL/anti-HEL model does not alter anergy or serum anti-HEL Ab and question the role for NFATs in B cell tolerance (Winslow *et al.*, 2006). Our data suggest that one of the consequences of NFATc2's actions is to prevent the induction of NFATc1 following BCR stimulation. NFATc1 is known to support proliferation and suppress activation-induced cell death in B cells upon BCR stimulation (Bhattacharyya *et al.*, 2011). Thus, elimination of calcineurin b1, necessary for NFATc1 activation, may mask some of the tolerogenic actions of NFATc2 and help explain alternative outcomes in the different experimental systems.

Global elimination of B cells with therapies such as anti-CD20 is emerging as an important means of intervention in serious autoimmune diseases. The success of these approaches also identifies the B cell repertoire as a potential target for early intervention to prevent autoimmune disease in high risk individuals (Silverman and Weisman, 2003). Selective elimination of important B cell specificities without total depletion of the repertoire is a highly attractive goal for the future. Such a goal may be similarly achieved by understanding and fine tuning the mechanisms of B cell tolerance so that key autoreactive B cells can be inactivated or removed from the repertoire. Similarly, overzealous tolerance mechanisms may introduce a barrier for effective vaccines, and understanding how to relieve this barrier could enhance vaccine design. The NFAT family of transcription factors resides at the interface of signals that promote either activation or tolerance; as such, NFATs are uniquely suited as a means to modify tolerance thresholds. Our findings support the concept that NFATc2 has a subtle but specific role in BCR anergy by regulating the responses of other NFATs (NFATc1 and NFATc3). Further studies are necessary to elucidate the roles of alternative spliced NFAT isoforms and their gene targets in modifying the balance between activation and unresponsiveness in anti-insulin B cells.

Acknowledgments

Abbreviations

Ab	Antibody
BCR	B cell receptor
FBS	Fetal bovine serum
FO	Follicular
HBSS	Hanks buffered salt solution
HEL	Hen egg lysozyme
MFI	Mean fluorescence intensity
MZ	Marginal zone
NOD	nonobese diabetic mouse
T1	Transitional 1
T1D	Type 1 diabetes
TD	T cell-dependent

References

Acevedo-Suarez CA, Hulbert C, Woodward EJ, Thomas JW. Uncoupling of anergy from developmental arrest in anti-insulin B cells supports the development of autoimmune diabetes. J. Immunol. 2005; 174:827–833. [PubMed: 15634904]

Acevedo-Suarez CA, Kilkenny DM, Reich MBTJ. Impaired Intracellular Calcium Mobilization and NFATc1 Availability in Tolerant Anti-Insulin B cells. J Immunol. 2006; 177:2234–2241. [PubMed: 16887983]

Barrington RA, Borde M, Rao A, Carroll MC. Involvement of NFAT1 in B cell self-tolerance. J Immunol. 2006; 177:1510–1515. [PubMed: 16849457]

Bell SE, Goodnow CC. A selective defect in IgM antigen receptor synthesis and transport causes loss of cell surface IgM expression on tolerant B lymphocytes. EMBO J. 1994; 13:816–826. [PubMed: 8112296]

Bhattacharyya S, Deb J, Patra AK, Thuy Pham DA, Chen W, Vaeth M, Berberich-Siebelt F, Klein-Hessling S, Lamperti ED, Reifenberg K, Jellusova J, Schweizer A, Nitschke L, Leich E, Rosenwald A, Brunner C, Engelmann S, Bommhardt U, Avots A, Muller MR, Kondo E, Serfling E. NFATc1 affects mouse splenic B cell function by controlling the calcineurin--NFAT signaling network. J. Exp. Med. 2011; 208:823–839. [PubMed: 21464221]

Blackshear J, Rotner HE, Kriauciunas KAM, Kahn CR. Reactive hypoglycemia and insulin autoantibodies in drug-induced lupus erythematosus. Ann Intern Med. 1983; 99:182–184. [PubMed: 6349454]

Chuvpilo S, Avots A, Berberich-Siebelt F, Glockner J, Fischer C, Kerstan A, Escher C, Inashkina I, Hlubek F, Jankevics E, Brabletz T, Serfling E. Multiple NF-ATc isoforms with individual transcriptional properties are synthesized in T lymphocytes. J. Immunol. 1999; 162:7294–7301. [PubMed: 10358178]

Coutinho A, Kazatchkine MD, Avrameas S. Natural autoantibodies. Curr. Opin. Immunol. 1995; 7:812–818. [PubMed: 8679125]

Dolmetsch RE, Lewis RS, Goodnow CC, Healy JI. Differential activation of transcription factors induced by Ca2+ response amplitude and duration. Nature. 1997; 386:855–858. [PubMed: 9126747]

Eisenbarth GS, Moriyama H, Robles DT, Liu E, Yu L, Babu S, Redondo M, Gottlieb P, Wegmann D, Rewers M. Insulin autoimmunity: prediction/precipitation/prevention type 1A diabetes. Autoimmun. Rev. 2002; 1:139–145. [PubMed: 12849007]

Goodnow CC. Transgenic mice and analysis of B-cell tolerance. Annu Rev Immunol. 1992; 10:489–518. [PubMed: 1590994]

Henry RA, cevedo-Suarez CA, Thomas JW. Functional silencing is initiated and maintained in immature anti-insulin B cells. J. Immunol. 2009; 182:3432–3439. [PubMed: 19265121]

Henry-Bonami RA, Williams JM, Rachakonda AB, Karamali M, Kendall PL, Thomas JW. B lymphocyte "original sin" in the bone marrow enhances islet autoreactivity in type 1 diabetes-prone nonobese diabetic mice. J. Immunol. 2013; 190:5992–6003. [PubMed: 23677466]

Hodge MR, Ranger AM, Charles dlB, Hoey T, Grusby MJ, Glimcher LH. Hyperproliferation and dysregulation of IL-4 expression in NF-ATp-deficient mice. Immunity. 1996; 4:397–405. [PubMed: 8612134]

Keck K. Ir gene control of immunogenicity of insulin and A chain loop as a carrier determinant. Nature. 1975; 254:78–79. [PubMed: 46593]

Kendall PL, Case JB, Sullivan AM, Holderness JS, Wells KS, Liu E, Thomas JW. Tolerant anti-insulin B cells are effective APCs. J. Immunol. 2013; 190:2519–2526. [PubMed: 23396943]

Kendall PL, Woodward EJ, Hulbert C, Thomas JW. Peritoneal B cells govern the outcome of diabetes in non-obese diabetic mice. Eur. J. Immunol. 2004; 34:2387–2395. [PubMed: 15307171]

Lupsa BC, Chong AY, Cochran EK, Soos MA, Semple RK, Gorden P. Autoimmune forms of hypoglycemia. Medicine (Baltimore). 2009; 88:141–153. [PubMed: 19440117]

Macian F, Garcia-Cozar F, Im SH, Horton HF, Byrne MC, Rao A. Transcriptional mechanisms underlying lymphocyte tolerance. Cell. 2002; 109:719–731. [PubMed: 12086671]

Palmer JP, Asplin CA, Clemons P, Lyen K, Tatpati O, Raghu PK, Paguette TC. Insulin antibodies in insulin-dependent diabetes before insulin treatment. Science. 1983; 222:1337–1339. [PubMed: 6362005]

Rojas M, Hulbert C, Thomas JW. Anergy and not clonal ignorance determines the fate of B cells that recognize a physiological autoantigen. J Immunol. 2001; 166:3194–3200. [PubMed: 11207272]

Silverman GJ, Weisman S. Rituximab therapy and autoimmune disorders: prospects for anti-B cell therapy. Arthritis Rheum. 2003; 48:1484–1492. [PubMed: 12794814]

van Haeften TW. Clinical significance of insulin antibodies in insulin-treated diabetic patients. Diabetes Care. 1989; 12:641–648. [PubMed: 2676431]

Winslow MM, Gallo EM, Neilson JR, Crabtree GR. The calcineurin phosphatase complex modulates immunogenic B cell responses. Immunity. 2006; 24:141–152. [PubMed: 16473827]

Xanthoudakis S, Viola JP, Shaw KT, Luo C, Wallace JD, Bozza PT, Luk DC, Curran T, Rao A. An enhanced immune response in mice lacking the transcription factor NFAT1. Science. 1996; 272:892–895. [PubMed: 8629027]

Highlights

- Functional inactivation of NFATc2 does not alter the production or maturation of anti-insulin B cells into follicular or marginal zone B cells.

- Insulin antibody production remains silenced in the absence of NFATc2.

- NFATc2 regulates anergy in anti-insulin B cells following BCR stimulation.

- Lifting anergy in NFATc2$^{-/-}$ anti-insulin B cells is associated increased transcription of NFATc1 and NFATc3.
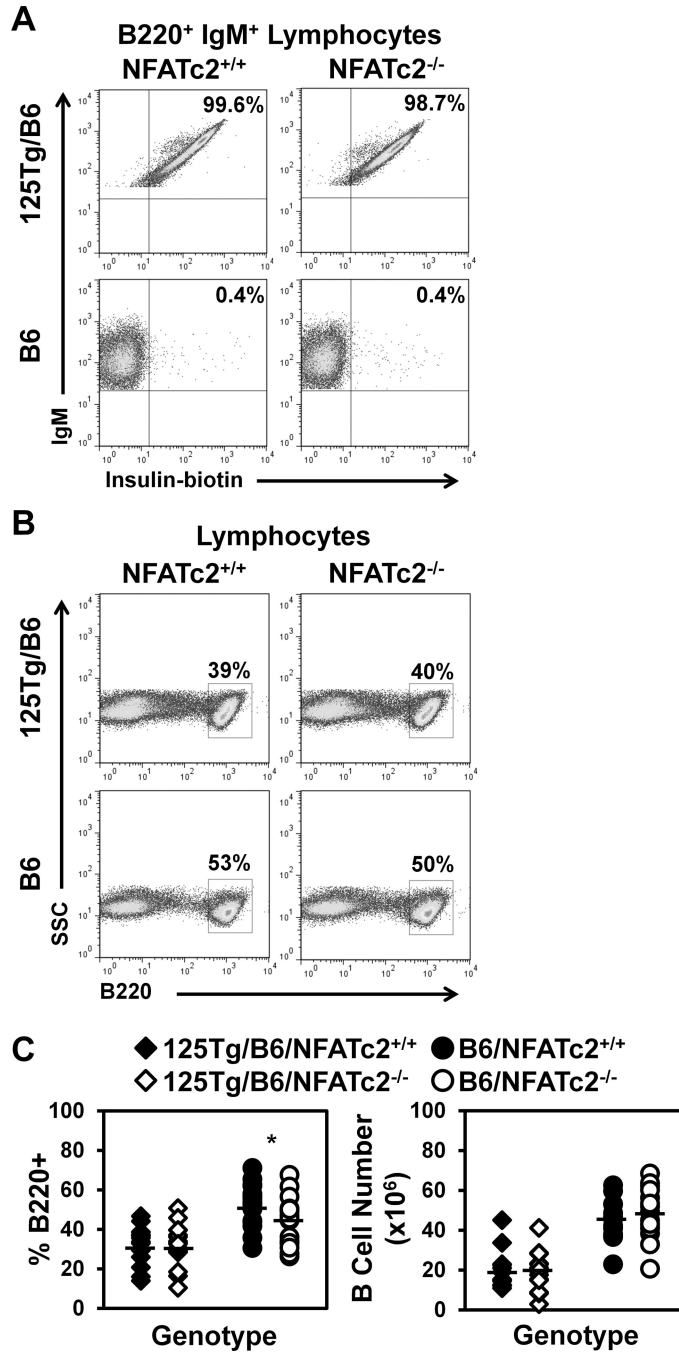
Figure 1. Loss of NFATc2 does not alter the percentage or number of insulin-binding B cells in the spleen

B220, IgM, and insulin-reactivity were assessed in freshly isolated splenocytes using flow cytometry. (A) The frequency of insulin-binding B cells was assessed in 125Tg/B6 (top) or B6 (bottom), NFATc2^{+/+} (left) or NFATc2^{−/−} (right) B220[+] IgM[+] lymphocytes. (B) The frequency of B220^{+} cells was assessed in 125Tg/B6 (top) or B6 (bottom), NFATc2^{+/+} (left) or NFATc2^{−/−} (right) lymphocyte gated splenocytes. (C) Summary of n   14 individual mice for each genotype; 125Tg/B6/NFATc2^{+/+} (black diamonds), 125Tg/B6/NFATc2^{−/−} (white diamonds), B6/NFATc2^{+/+} (black circles), B6/NFATc2^{−/−} (white circles). B cells

gated as in (B), B cell percentages, left, B cell numbers, right. A two-tailed t-test was used to compare NFATc2$^{+/+}$ vs. NFATc2$^{-/-}$ mice, * $p < 0.05$.
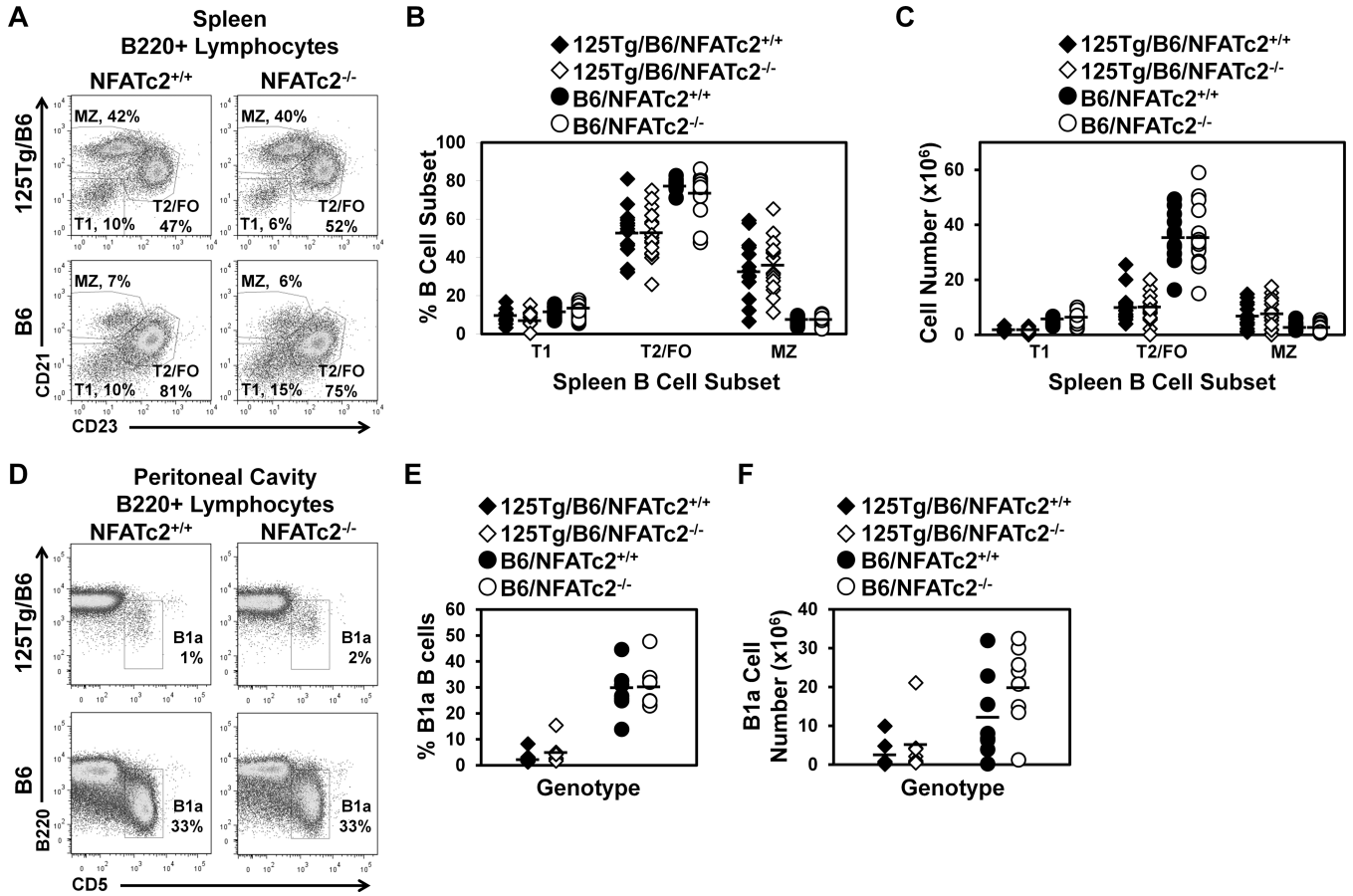
Figure 2. Subsets of peripheral B cells are not affected by NFATc2 deficiency

(A–C) Freshly isolated splenocytes were harvested and flow cytometry was used to identify B220$^+$ lymphocytes. (A) Representative dot plots indicate the frequency of each B cell subset. CD21 and CD23 expression define T1 (CD21^{low} CD23^{low}), T2/FO (CD21^{low} CD23^{high}), and MZ (CD21high CD23^{low}) B cells in 125Tg/B6 (top) or B6 (bottom) NFATc2$^{+/+}$ (left) or NFATc2$^{-/-}$ (right) lymphocyte gated splenocytes. (B–C) Summary of percentages (B) or numbers (C) of B cell subsets identified as in (A) of n   14 mice of each genotype; 125Tg/B6/NFATc2$^{+/+}$ (black diamonds), 125Tg/B6/NFATc2$^{-/-}$ (white diamonds), B6/NFATc2$^{+/+}$ (black circles), B6/NFATc2$^{-/-}$ (white circles). (D–F) The frequency of B1a B cells (B220^{low} CD5$^+$) in peritoneal cavity lavage was assessed using flow cytometry. (D) Representative dot plots are gated on B220$^+$ lymphocytes. (E–F) Summary of the percentage (E) or number (F) of B1a cells in n   7 mice of each genotype; 125Tg/B6/NFATc2$^{+/+}$ (black diamonds), 125Tg/B6/NFATc2$^{-/-}$ (white diamonds), B6/ NFATc2$^{+/+}$ (black circles), B6/NFATc2$^{-/-}$ (white circles). A two-tailed t-test showed no significant differences conferred by inactivation of NFATc2 in any of the subsets examined.

A
125Tg/B6

B
B6
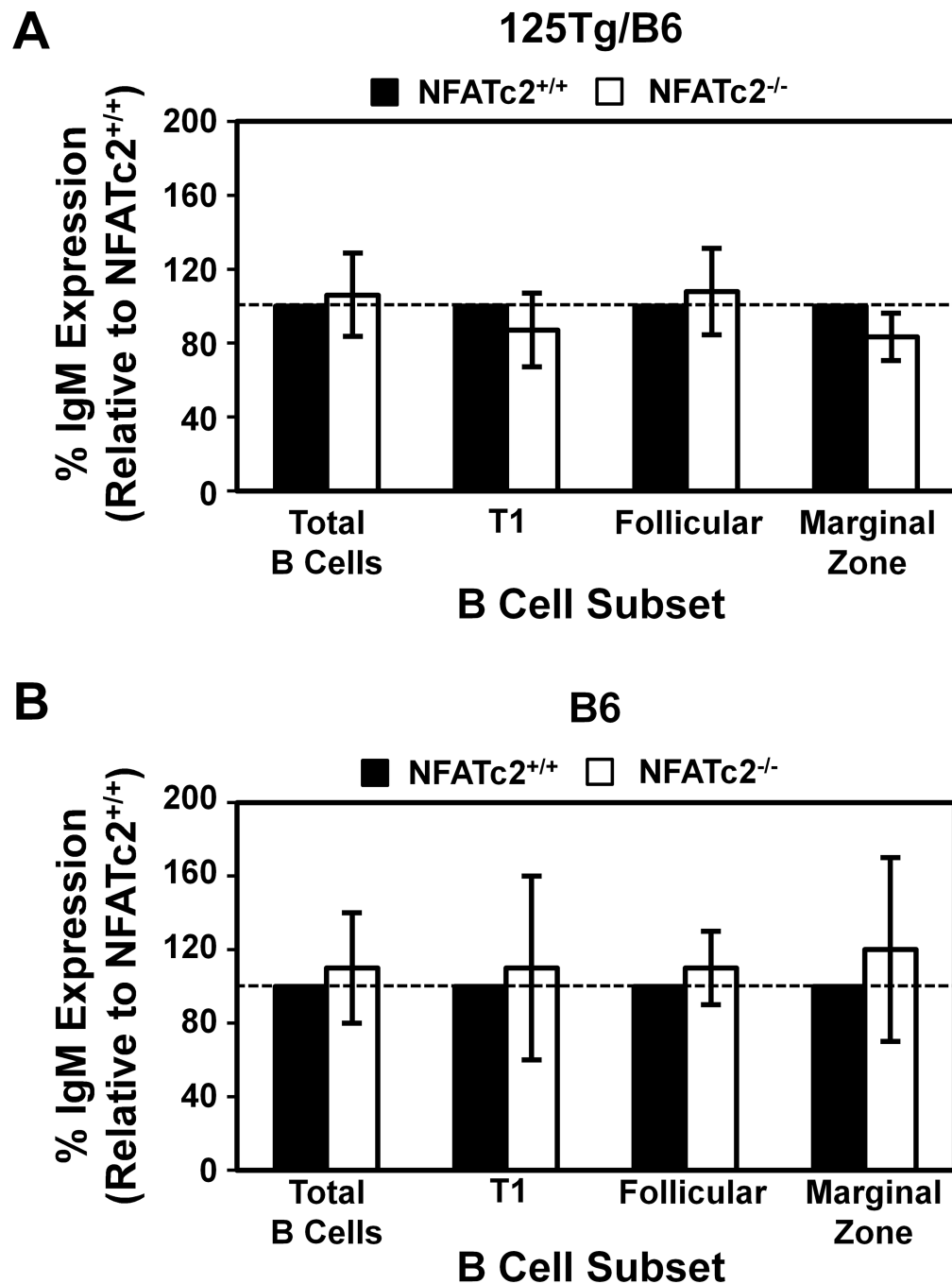
Figure 3. B cell receptor surface expression is not altered by loss of NFATc2
Freshly isolated splenocytes were harvested and flow cytometry was used to identify B220+
lymphocytes. T1, T2/FO, and MZ B cell subsets were identified as in Fig. 2. The IgM MFI
of NFATc2$^{-/-}$ B cells was divided by the IgM MFI of NFATc2$^{+/+}$ B cells within each subset
indicated (white bars), such that NFATc2$^{+/+}$ IgM relative expression was set to 100% (black
bars, shown as reference). The % IgM expression average ± standard deviation is shown for
125Tg/B6 (A) or B6 (B) NFATc2$^{-/-}$ mice; n ≥ 6 mice for each genotype. Dashed line
indicates 100% (i.e. no change). A one sample, two-tailed t-test showed no statistically

significant differences between the indicated B cell subsets of NFATc2$^{-/-}$ mice relative to 100% IgM expression of NFATc2$^{+/+}$ mice.

A

B
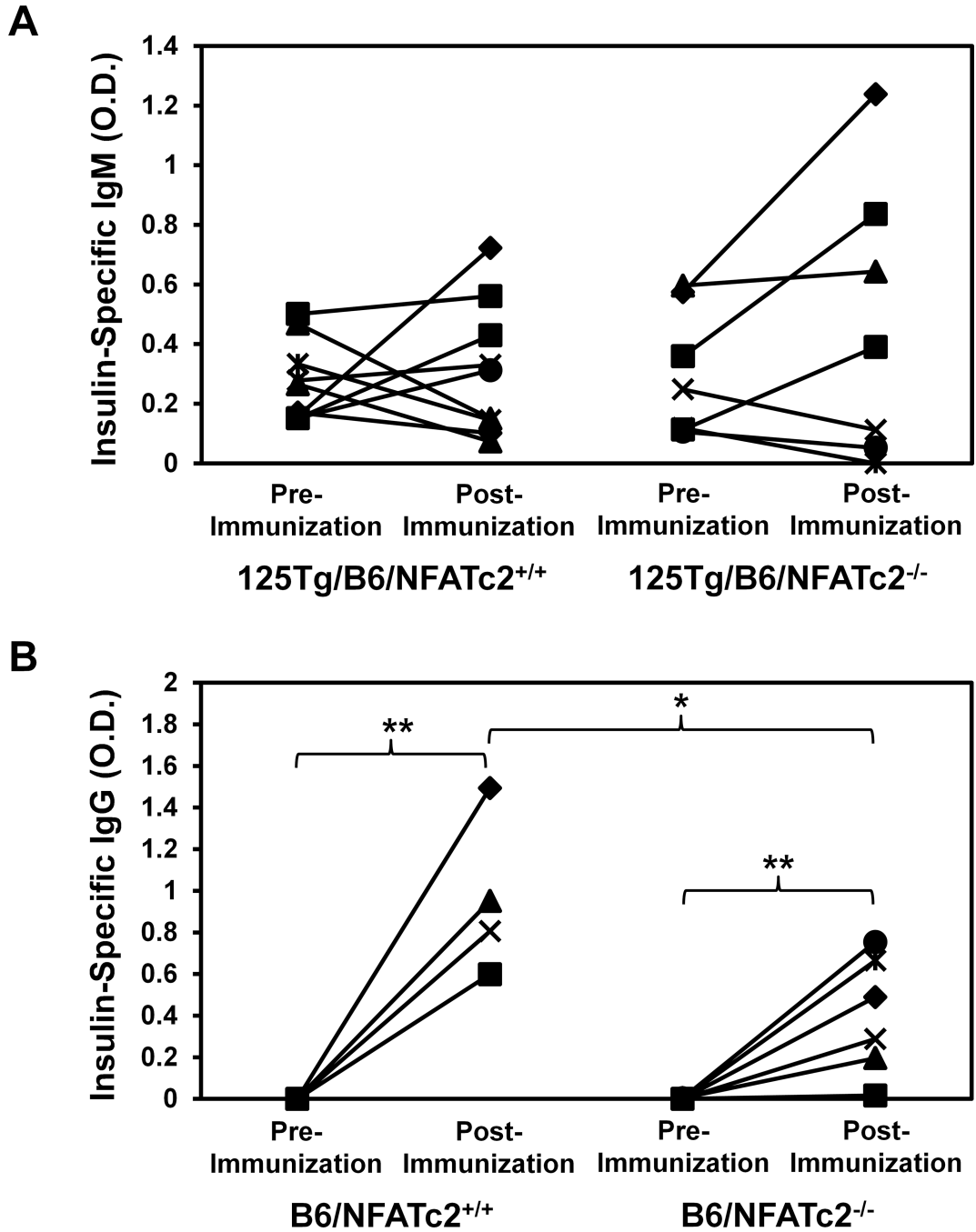
Figure 4. Functional inactivation of NFATc2 does not enhance insulin antibody production following T cell-dependent immunization

Mice were immunized subcutaneously with beef insulin in CFA. Pre-immune and 2 weeks post-immunization sera were harvested and ELISA was used to measure the insulin-specific O.D. 405 nm as in Methods. (A) Pre-immunization and post-immunization IgM insulin-specific binding is compared in 125Tg/B6/NFATc2$^{+/+}$ (left, n = 9) and 125Tg/B6/NFATc2$^{-/-}$ mice (right, n = 7). (B) Pre-immunization and post-immunization IgG insulin-specific binding is compared in B6/NFATc2$^{+/+}$ (left, n = 4) and B6/NFATc2$^{-/-}$ mice (right, n = 6). Pre vs. post-immunization data were compared for each genotype, and pre (or post)-

immunization was also compared between NFATc2$^{-/-}$ vs. NFATc2$^{+/+}$ mice; * p = 0.05, ** p < 0.01 by two-tailed t-test;
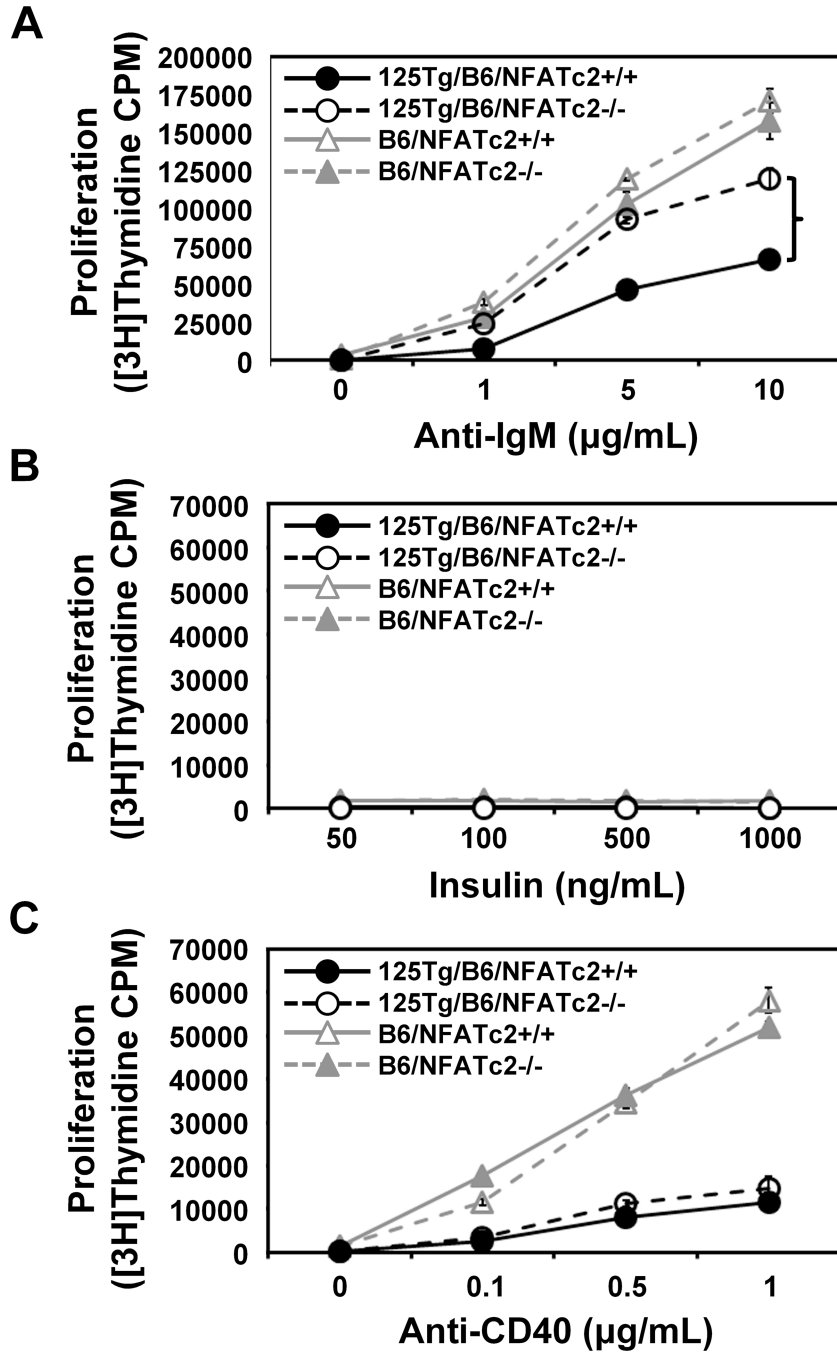
Figure 5. Loss of functional NFATc2 relieves anergy in anti-insulin B cells following BCR, but not anti-CD40 stimulation

Purified B cells (see Methods) were incubated with the concentration of anti-IgM F(ab')$_2$ (T-independent, panel A), insulin (T-independent, panel B), or anti-CD40 (T-dependent, panel C) indicated. Proliferation was assessed by measuring [3H]Thymidine incorporation; the average of triplicate wells ± SD is shown. This cohort includes 8 mice, two pooled from each genotype; 125Tg/B6/NFATc2$^{+/+}$ (black circles, solid black line), 125Tg/B6/ NFATc2$^{-/-}$ (open circles, dashed black line), B6/NFATc2$^{+/+}$ (grey triangles, solid grey line), and B6/NFATc2$^{-/-}$ B cells (open triangles, dashed grey line). NFATc2$^{+/+}$ and

NFATc2$^{-/-}$ responses following stimulation were compared using a Wilcoxon rank-sum test, * $p < 0.05$. Data are representative of 2 experiments.
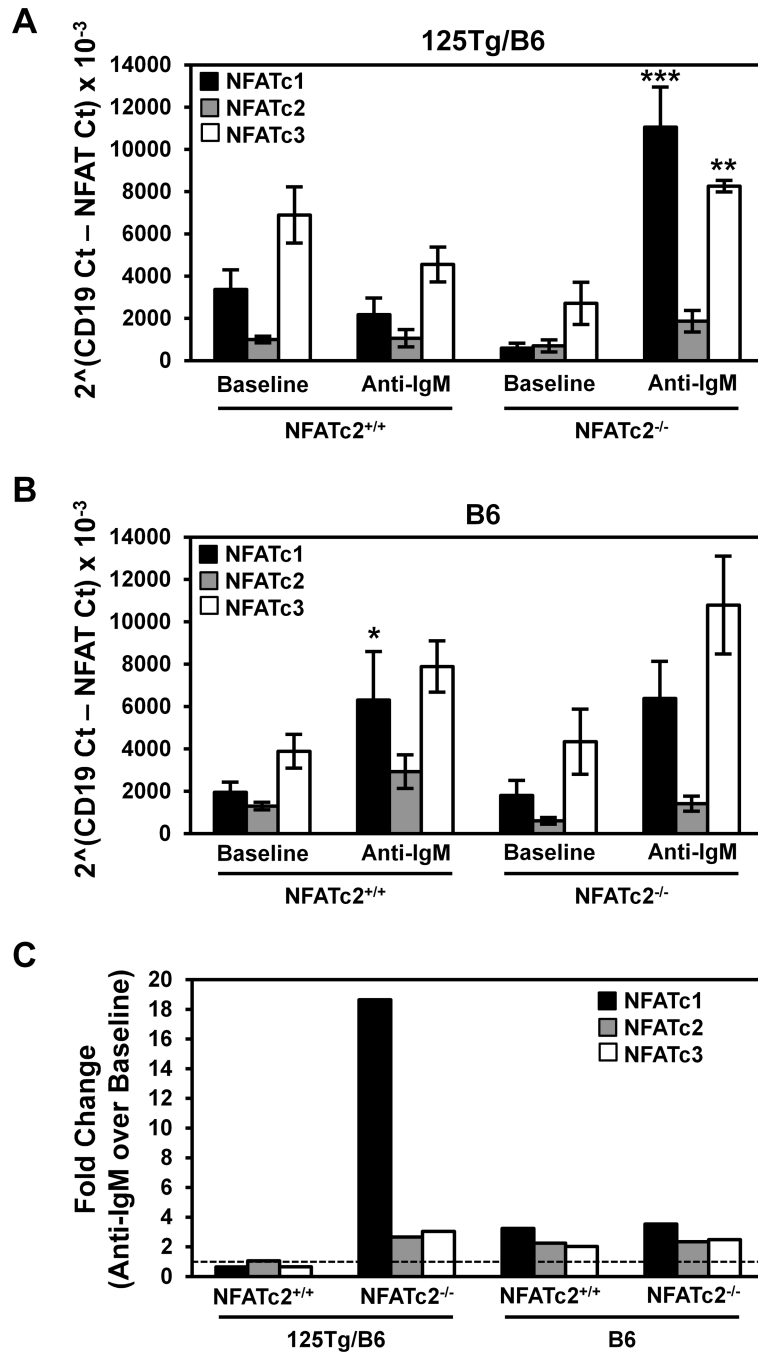
Figure 6. BCR-stimulated *NFATc1* and *NFATc3* expression is increased when functional NFATc2 expression is lost

B cells were purified (see Methods) from 125Tg/B6 or B6 NFATc2$^{+/+}$ or NFATc2$^{-/-}$ mice and were stimulated for 1h at 37°C with or without 10 μg/mL anti-IgM F(ab')$_2$. Real-time PCR was used to assess the levels of *NFATc1*, *NFATc2*, and *NFATc3* transcripts at baseline or following stimulation with anti- IgM F(ab')$_2$. *NFAT* Ct values were normalized to *CD19* transcript levels [2^(CD19 Ct- NFAT Ct)]. Average ± SEM is shown for (A) 125Tg/B6 or (B) B6 mice, n = 3–9 mice in each genotype, n = 3 experiments; * p < 0.05, ** p < 0.01, *** p < 0.001, as calculated by Wilcoxon rank-sum test comparison of anti-IgM stimulation with

baseline data for a given *NFAT* species within each genotype. (C) The fold change of anti-IgM over baseline data in A–B was calculated for each NFAT species within each genotype. The dashed line indicates no change.

Table 1

Percentage of B cell subsets in the spleen

	% B Cells[a]	% T1[b]	% T2/Follicular[b]	% Marginal Zone[b]
125Tg/B6/NFATc2^{+/+}	32 ± 9	9.2 ± 3.3	52 ± 14	35 ± 15
125Tg/B6/NFATc2^{−/−}	32 ± 10	7.6 ± 3.3	53 ± 13	36 ± 14
p value[c]	0.96	0.19	0.92	0.82
B6/NFATc2^{+/+}	52 ± 11	11 ± 3	77 ± 4	7.1 ± 1.8
B6/NFATc2^{−/−}	44 ± 12	12 ± 4	72 ± 10	6.9 ± 2.8
p value[c]	0.04	0.33	0.06	0.86

[a]Gated on B220[+] lymphocytes, percentage of lymphocyte gate shown.

[b]Subsets defined using CD21 and CD23 expression as in Fig. 2, percentage of B220[+] lymphocytes shown.

[c]Calculated using a two-tailed t test, n 14 mice.

Table 2

Number of B cell subsets in the spleen

	Total B Cell Number[a] (×10⁶ cells)	T1[b] (×10⁶ cells)	T2/Follicular[b] (×10⁶ cells)	Marginal Zone[b] (×10⁶ cells)
125Tg/B6/NFATc2$^{+/+}$	19 ± 9	1.6 ± 0.6	9.9 ± 5.7	6.8 ± 4.4
125Tg/B6/NFATc2$^{-/-}$	20 ± 10	1.5 ± 0.9	9.4 ± 5.1	7.4 ± 5.4
p value[c]	0.74	0.71	0.79	0.75
B6/NFATc2$^{+/+}$	45 ± 10	4.8 ± 1.3	35 ± 9	3.1 ± 1.2
B6/NFATc2$^{-/-}$	49 ± 13	5.4 ± 2.3	36 ± 11	3.2 ± 1.5
p value[c]	0.45	0.44	0.91	0.92

[a] Gated on B220$^+$ lymphocytes.

[b] B220$^+$ lymphocyte subsets identified using CD21 and CD23 expression as in Fig. 2.

[c] Calculated using a two-tailed t test, n ≤ 14 mice.

Table 3

Percentage and number of B1a B cells in the peritoneal cavity

	%B1a B cells[a, b]	B1a Cell Number[a] ($\times 10^4$ cells)
125Tg/B6/NFATc2$^{+/+}$	2.9 ± 2.5	2.4 ± 3.7
125Tg/B6/ NFATc2$^{-/-}$	5.1 ± 4.7	4.8 ± 7.4
p value[c]	0.30	0.45
B6/NFATc2$^{+/+}$	29 ± 9	12 ± 11
B6/NFATc2$^{-/-}$	29 ± 9	20 ± 10
p value[c]	0.95	0.13

[a]B1a identified as B220^{low} CD5^{+} lymphocytes.

[b]Percentage of B220^{+} lymphocyte gate shown.

[c]Calculated using a two-tailed t test, n 7 mice.